CHAPTER 3

Growth and Characterization of Copper Indium Diselenide (CIS) compound and its Thin Films as an Absorber Layer

3. Growth and Characterization of Copper Indium Diselenide (CIS) Compound and its Thin Films as an Absorber Layer

Polycrystalline copper indium diselenide (CIS) thin films and its' related quaternary compounds such as copper indium gallium diselenide (CIGS) are considered almost ideal compound semiconductor materials for thin film photovoltaic applications. This fact is clearly demonstrated by reported high conversion efficiencies close to 20 % for laboratory scale cells based on CIGS [22] and around 13 % for mini modules [83]. The chalcopyrite absorber materials of these high efficiency devices are generally produced by a single stage growth technique in which all the elements (i.e. Cu, In, Ga and Se) are co-evaporated from individual sources. This technique requires accurate control of all evaporation sources to deposit CIS/CIGS thin films. As an alternative, several relatively simple low cost deposition techniques are under active study [84,85,86,87,88,89]. Thermal and flash evaporation techniques to deposit CIS thin films from synthesized absorber compound material are the useful techniques for the deposition of CIS and CIGS thin films.

In this study, we have first synthesized CIS compound material with different selenium concentration. Structural, compositional and morphological properties of synthesized pulverized CIS compound material are investigated. The CIS compound material having better structural and compositional properties is used as a source material to deposit CIS thin films, initially on glass substrates held at different substrate temperatures (T_s) for optimizing the deposition parameters and then on the molybdenum coated glass substrates for fabrication of CIS based solar cell the device.

In thermal evaporation technique, the CIS thin films are prepared by evaporating fixed amount of pulverized compound material from single evaporation source over a relatively short period of time (~10 min). The crystalline quality and in-depth compositional uniformity of these thin films are critically influenced by T_s during growth. Films deposited at various T_s are thermally annealed at 573 K temperature. It will be indicated that by optimizing T_s, and thermal annealing of films at 573 K temperature, this

relatively simple, growth process produced single-phase CIS thin films with crystalline quality suitable for solar cell applications.

Flash evaporation is a well known technique especially useful for the evaporation of ternary or quaternary compounds and is first employed for CIS deposition over twenty years ago. This technique entails the transport of pulverized compound materials via a feeder to a heated evaporation source. In order to avoid decomposition of the compounds and hence phase splitting, very small amounts of material is slowly transported to the evaporation source kept well above the evaporation temperature of the compound. By following this procedure, the compound in the ideal case is evaporated prior to decomposition into separate phases. In this study, we have successfully deposited device quality CIS thin films by controlling the rate of deposition.

3.1 Synthesis of Copper Indium Diselenide Compound Material

Copper indium diselenide ($CuInSe_x$) compound is synthesized by mixing the individual elements i.e. copper, indium and selenium in 1:1:2 weight proportions with different selenium (Se) composition viz. x = 2, 2.05, and 2.1, in evacuated quartz ampoules. The melting of elements mixed in ampoule is then carried out in an electric furnace at heating rate of 3 K/min up to 1400 K. To ensure homogeneity of the melt holding at 1400 K is carried out for three hours. The melt is then cooled down to room temperature inside the furnace at a cooling rate of 4 K/min. The solid ingot is then powdered to a mean particle size of ~100 μm using the process of grinding and then sieving.

3.2 Properties of Synthesized $CuInSe_x$ Powders

3.2.1 Structural Properties

The X-ray diffraction (XRD) patterns of synthesized $CuInSe_x$ compound with different Se concentrations are shown in figure 3.1. The analysis of XRD data show that synthesized compound material having different Se concentrations are polycrystalline in nature. The absence of XRD peaks due to binary alloy or different phases and reflections only typical of CIS compound material in the XRD spectra confirms that the single phase chalcopyrite material is formed. The (112) preferred orientation of grains and splitting of peaks due to

tetragonal structure demonstrate good crystalline quality and structural homogeneity of synthesized compound.

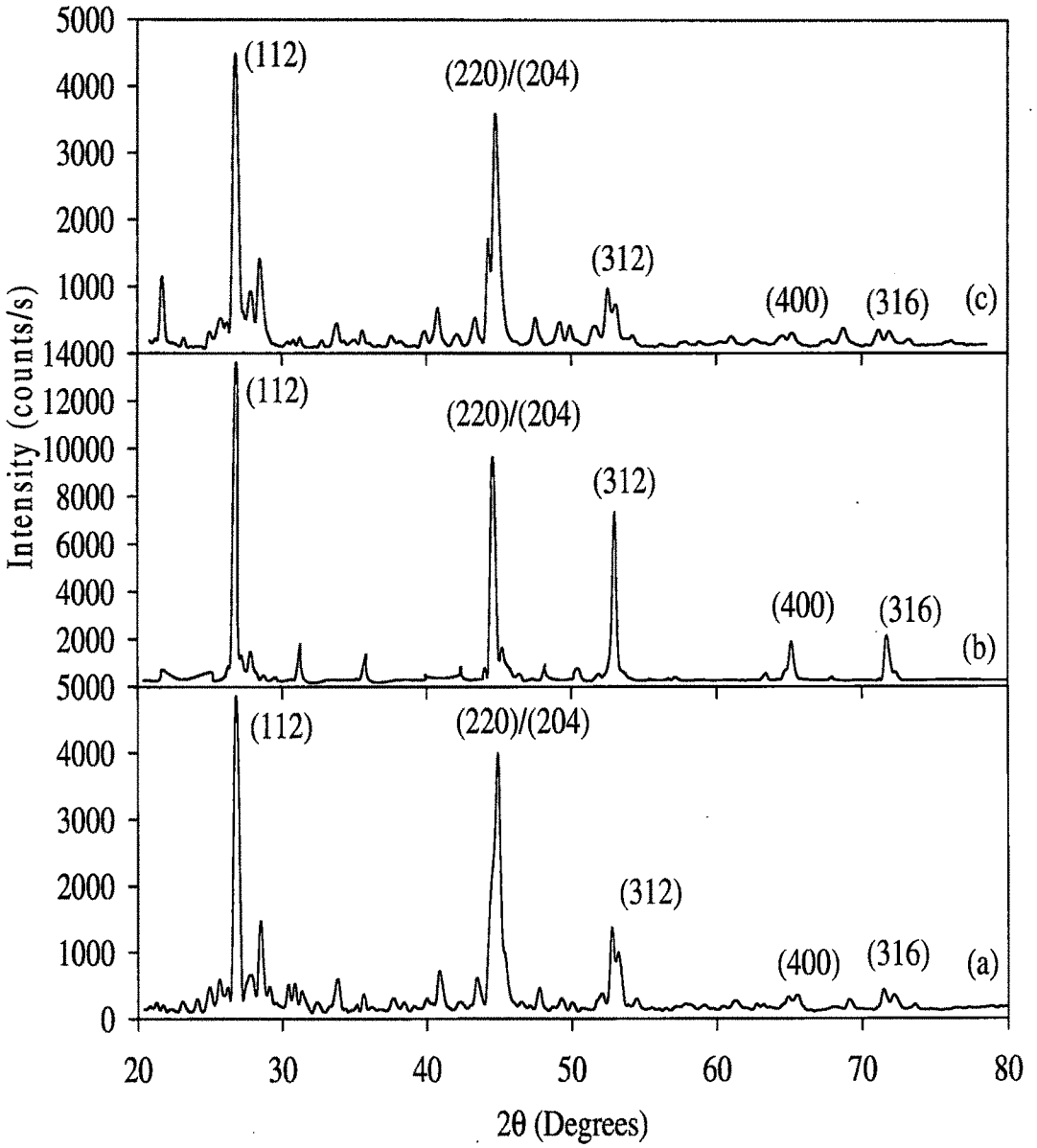

Figure 3.1: XRD patterns of synthesized $CuInSe_x$ compound material (a) x = 2, (b) x = 2.05, and (c) x = 2.1.

The lattice parameters a and c of synthesized bulk materials calculated from the interplanar spacing (d) for different selenium concentrations are shown in table 3.1. From the table, it is seen that a and c values are varying nonlinearly with selenium concentration. $CuInSe_x$ compound having x = 2.05 have values of a and c in close agreement with the American Society for Testing and Materials (ASTM) values (viz. a = 0.5782 nm and c = 1.1619 nm).

Table 3.1: Lattice parameters of synthesized $CuInSe_x$ compound with different values of x.

x (wt.%)	a (nm)	c (nm)	$\eta = c/2a$
2	0.5754	1.2040	1.0462
2.05	0.5801	1.1596	0.9994
2.10	0.5753	1.2033	1.0458

The calculated lattice parameters are utilized to estimate free parameter (u) and I-VI, III-VI bond lengths using the Abrahams-Bernstein relations [90]. Table 3.2 shows the values of u, I-VI, III-VI bond lengths and tetragonal distortion (2-c/a). It is seen that the u is close to ideal value of 0.25 for x = 2.05. The tetragonal distortion (2-c/a) is an important parameter in chalcopyrite compounds which results in a crystal field that lifts the degeneracy of the top-most valance band. From the table 3.2 it is observed that tetragonal distortion is almost zero for $CuInSe_x$ compound having x = 2.05.

Table 3.2: Free parameter (u), bond lengths ($d_{I\text{-}VI}$ and $d_{III\text{-}VI}$) and the tetragonal distortion [2-c/a] values for synthesized $CuInSe_x$ compound for different values of x.

x (wt.%)	Free parameter (u)	$d_{I\text{-}VI}$ (nm)	$d_{III\text{-}VI}$ (nm)	$2 - c/a$
2	0.228	0.246	0.261	-0.092
2.05	0.250	0.251	0.251	0.001
2.10	0.227	0.245	0.260	-0.091

The crystallite size of synthesized $CuInSe_x$ compound having different values of x is calculated using the well known Scherrer's formula after the correction for the instrumental spectral broadening. Here λ is the wavelength of Cu K_α radiation ($\lambda = 0.154056$ nm), B_r is the full width at half maximum (FWHM) of (112) peak. The peak position of (112) plane and FWHM of the (112) peak, along with the calculated values of the crystallite size, are shown in table 3.3. It is seen that the crystallite size increases with the increase in x. The scanning electron micrograph (SEM) images of synthesized $CuInSe_x$ compounds are shown in figure 3.2.

Table 3.3: The position of (112) peak, crystallite size and FWHM of synthesized $CuInSe_x$ compound.

x (wt.%)	Position of (112) peak (degrees)	FWHM (degrees)	Crystallite size, d (nm)
2	26.61	0.13	64
2.05	26.55	0.09	86
2.10	26.61	0.08	101

3.2.2 Composition of $CuInSe_x$ Powders

The composition of $CuInSe_x$ could be described by two parameters, non-molecularity and non-stoichiometry, which have been defined by Groenink and Janse [91] as parameters Δm and Δs. These parameters determine the deviation from molecularity and stoichiometry, respectively:

$$\Delta m = \frac{[Cu]}{[In]} - 1 \tag{3.1}$$

$$\Delta s = \frac{2[Se]}{[Cu]+3[In]} - 1 \tag{3.2}$$

The deviations of these parameters from zero indicate the following:

1. $\Delta m > 0 \Rightarrow$ synthesized compound material is Cu rich
   $\Delta m < 0 \Rightarrow$ synthesized compound material is In rich

2. $\Delta s > 0 \Rightarrow$ materials are with excess of selenium
   $\Delta s < 0 \Rightarrow$ materials are with selenium deficiency

In order to investigate the compositional analysis of the synthesized $CuInSe_x$ compounds EDAX analysis are carried out with an accelerating voltage of 30 kV using Se_L, In_L, and Cu_K line of the spectrum. EDAX spectrum of synthesized CIS material with varying selenium composition is shown in figure 3.3.

Table 3.4: EDAX analysis of synthesized $CuInSe_x$ compound.

x (wt. %)	Composition (wt. %)			Molecularity deviation Δm	Stoichiometry deviation Δs
	Cu	In	Se		
2	25.41	26.59	48.00	-0.040	0.91
2.05	25.50	24.74	50.26	0.030	1.02
2.10	25.36	24.76	49.88	0.037	0.97

EDAX results of composition of synthesized $CuInSe_x$ compound material with different Se concentrations, with the deviation from molecularity and deviation from stoichiometry, as calculated from the analysis of data of synthesized compound is shown in table 3.4. All the obtained results of EDAX measurements show that there is possibility to gain both-copper side and indium side deviations. Composition of $CuInSe_x$ compound grown without excess Se had Δm negative and Δm increased with increasing extra Se content. Adding extra Se of over 5 %, while mixing results in the positive values of Δm.

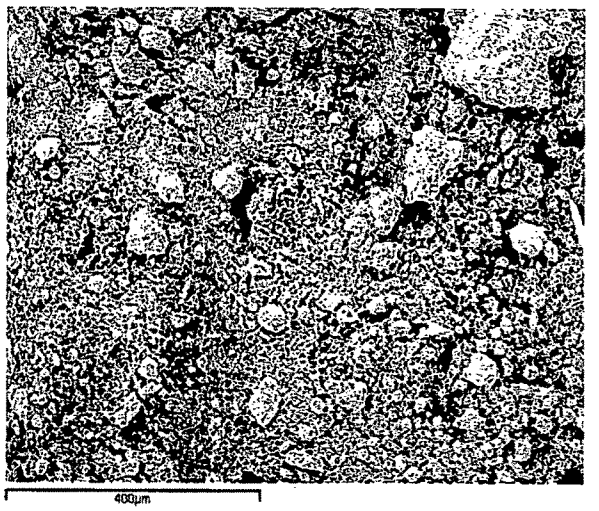

(a)

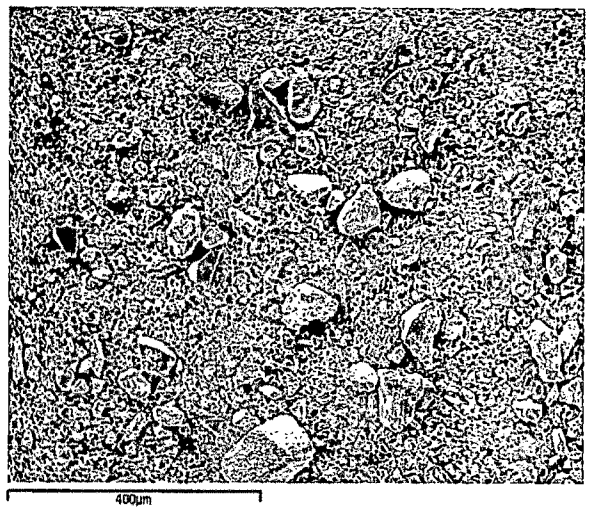

(b)

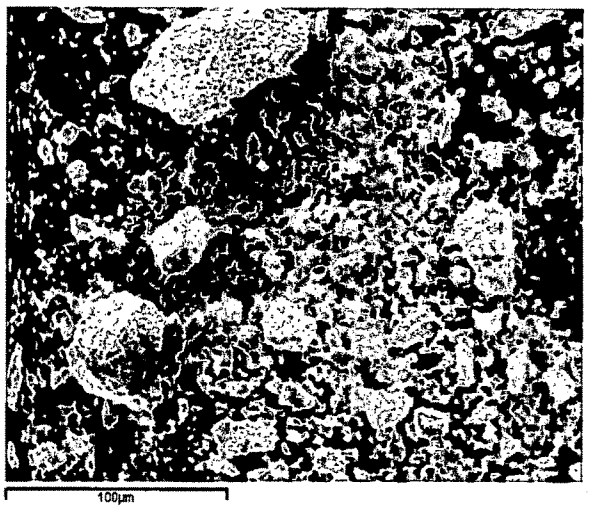

(c)

Figure 3.2: Scanning electron micrograph images of $CuInSe_x$ compound for different values of x: (a) x = 2, (b) x = 2.05 and (c) x = 2.10.

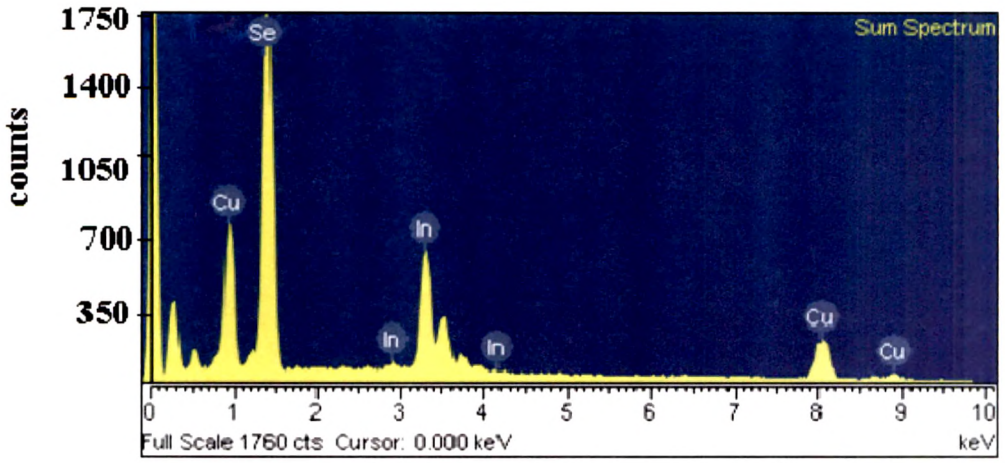

(a)

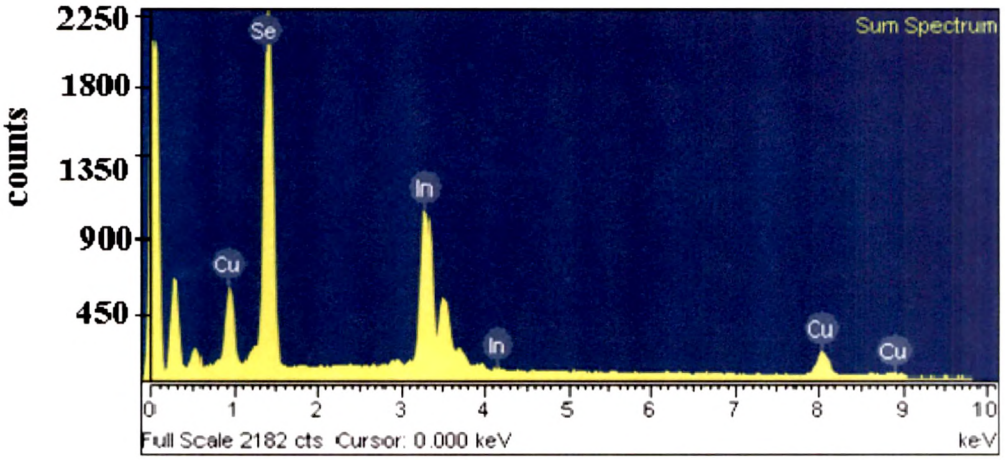

(b)

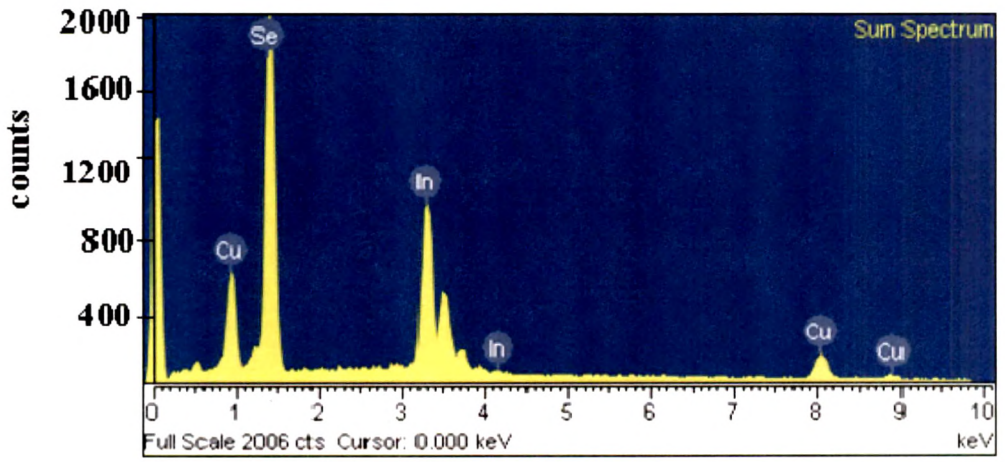

(c)

Figure 3.3: EDAX spectrum of $CuInSe_x$ compound for different values of x (a) x = 2, (b) x = 2.05 and (c) x = 2.10.

The detailed structural, morphological and compositional analysis of $CuInSe_x$ compound material indicates that synthesized CIS compound material having x = 2.05 is near stoichiometric alloy. As absorber layers prepared from such composition exhibited high open circuit voltages and efficiencies of more than 10 % [92], we have used it as a starting material to deposit CIS thin films.

3.3 Deposition of CIS Absorber Films

In this work, we have deposited CIS thin films on soda-lime glass substrates using two different techniques.

(1) Thermal evaporation of synthesized compound material by controlled increase in source temperature.
(2) Flash evaporation technique.

Results obtained using thermal evaporation technique is discussed in the section 3.4 while results of CIS thin films deposited using flash evaporation technique is discussed in the section 3.5.

3.4 Characterization of CIS Thin Films Deposited using Thermal Evaporation Technique

The chalcopyrite CIS thin films are prepared by thermal evaporation technique in which predetermined mass of synthesized pulverized chalcopyrite compound is placed on a single unheated evaporation source at room temperature. By a controlled increase in the source temperature under high-vacuum conditions, CIS thin films are initially deposited on glass substrates at different T_s (473 K-573 K) for optimization of the deposition parameters. Various characterizations carried out for as-deposited films are discussed here.

3.4.1 Structural Characterization of CIS Thin Films

Structural characterization of CIS films deposited at different T_s are carried out using XRD analysis in 2θ range 20°- 60° using Cu Kα radiation (λ = 0.150456 nm) and transmission electron microscopy with selected area diffraction pattern (SAD) to verify the exact structure.

3.4.1.1 Effect of Substrate Temperature

The XRD patterns carried out for CIS in powder form (with 5 % excess selenium) and thin films of CIS grown at three different T_s, viz 473 K, 523 K and 573 K is shown in figure 3.4. XRD analysis of films deposited at different T_s revealed that all films have an intense (112) preferred orientation of grains parallel to substrate.

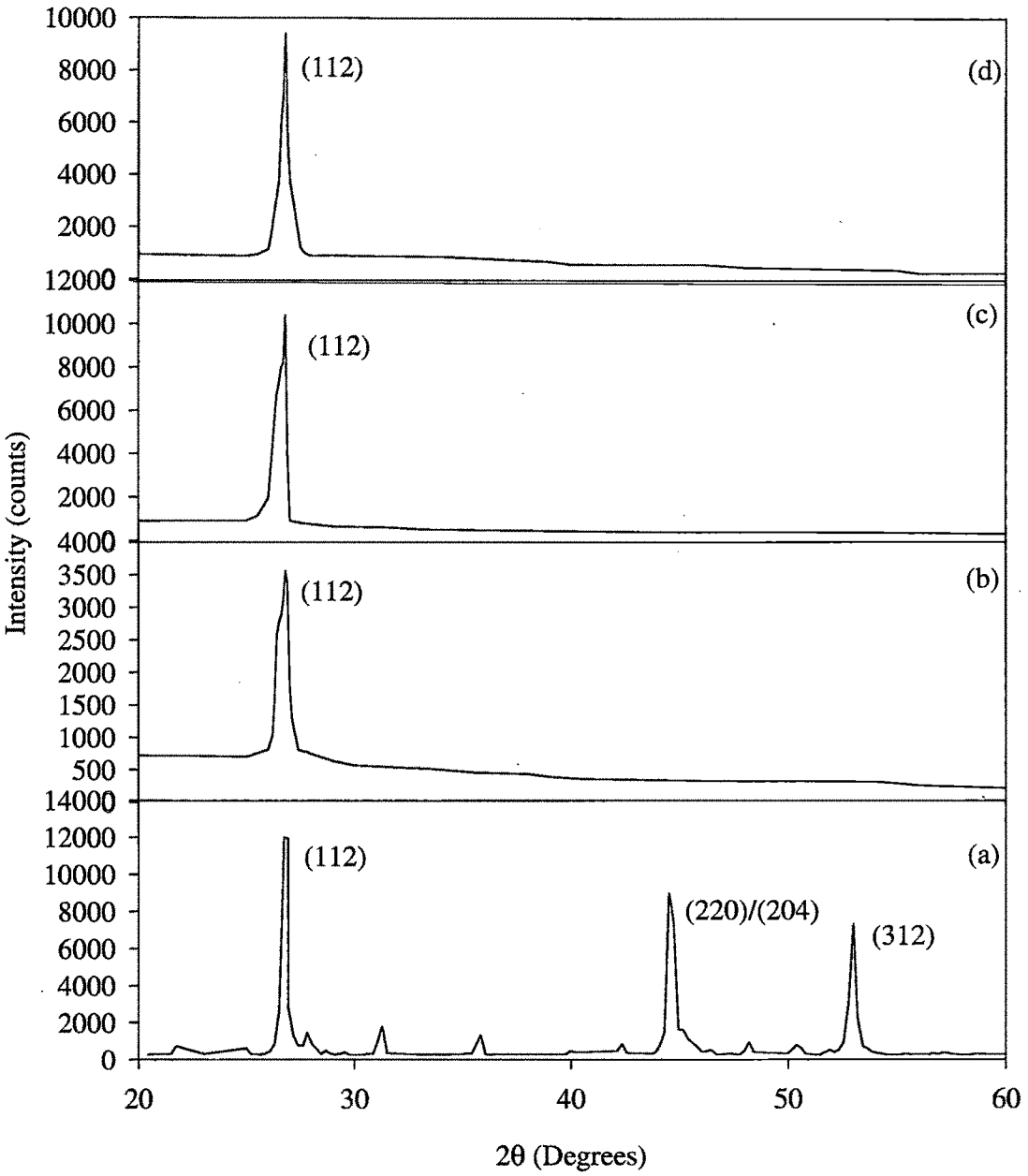

Figure 3.4: XRD patterns of (a) CIS powder and thin films deposited at (b) T_s = 473 K (c) T_s = 523 K, (d) T_s = 573 K.

However, the intensity of the diffraction line is highly dependent on T_s. CIS films deposited at low T_s resulted in a less intense diffraction line indicating that the film consists of micro-polycrystallites. A. A. S. Akl et al. [89] has also observed similar results for CIS films deposited using flash evaporation technique. At T_s = 573 K, the intensity of diffraction peak at $2\theta = 26.8°$ decreases. This may be due to selenium-deficient film as confirmed using EDAX results discussed in section 3.4.3.

3.4.1.2 Effect of Thermal Annealing

Thermal annealing of CIS thin films deposited at different T_s is carried out at 573 K, in vacuum coating unit at a base pressure of 10^{-2} Torr. The XRD spectrum of CIS in powder form and films deposited at different T_s and annealed at 573 K is shown in figure 3.5. It is observed that thermal annealing of the films increases the intensity of the (112) x-ray diffraction peak. However, no change in the orientation of the films is observed. A similar result has been observed by Benaicha et al. [93] for CIS thin films deposited using electrodeposition technique.

3.4.1.3 Crystallite Size

Crystallite size of the as deposited and annealed films is calculated using Scherrer's formula. The position and FWHM of the (112) peak, along with the calculated values of the crystallite size, for films grown at different T_s are shown in table 3.5. It is seen that the crystallite size increases with increase in T_s and annealing of CIS thin films. Similar results are obtained by other authors for as-deposited and annealed CIS thin films [86,94].

Table 3.5: The position of (112) peak, crystallite size and FWHM of CIS thin films grown at different substrate temperatures and annealed at 573 K.

Substrate Temperature T_s (K)	Annealing Temperature T_a (K)	Position of (112) peak 2θ (degrees)	FWHM (degrees)	Crystallite Size d (nm)
473	Unannealed	26.75	0.332	33
	573	26.75	0.266	45
523	Unannealed	26.70	0.249	51
	573	26.70	0.202	76
573	Unannealed	26.87	0. 309	36
	573	26.76	0.249	52

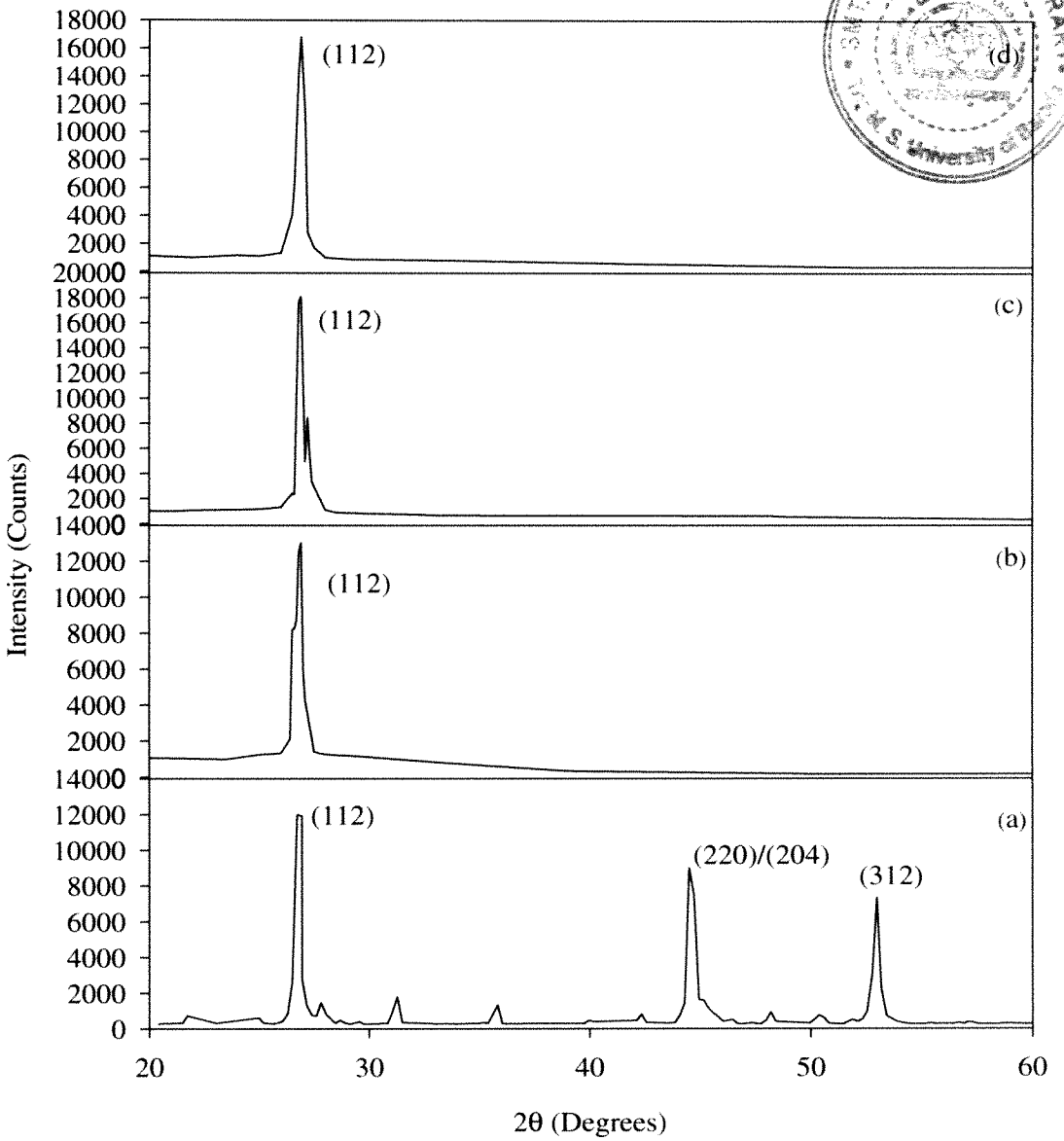

Figure 3.5: XRD patterns of (a) CIS powder and thin films deposited at (b) T_s = 473 K (c) T_s = 523 K, (d) T_s = 573 K and annealed at 573 K.

3.4.1.4 TEM Result

XRD analysis of CIS thin films deposited at different T_s and annealed at 573 K revealed that all films had (112) preferred orientation of grains. In order to confirm the exact structure of the CIS film, the structural analysis of film deposited at 523 K is carried out using TEM. The TEM image and typical selected area diffraction (SAD) pattern of representative CIS thin film (viz. Film deposited at 523 K) is shown in figure 3.6.

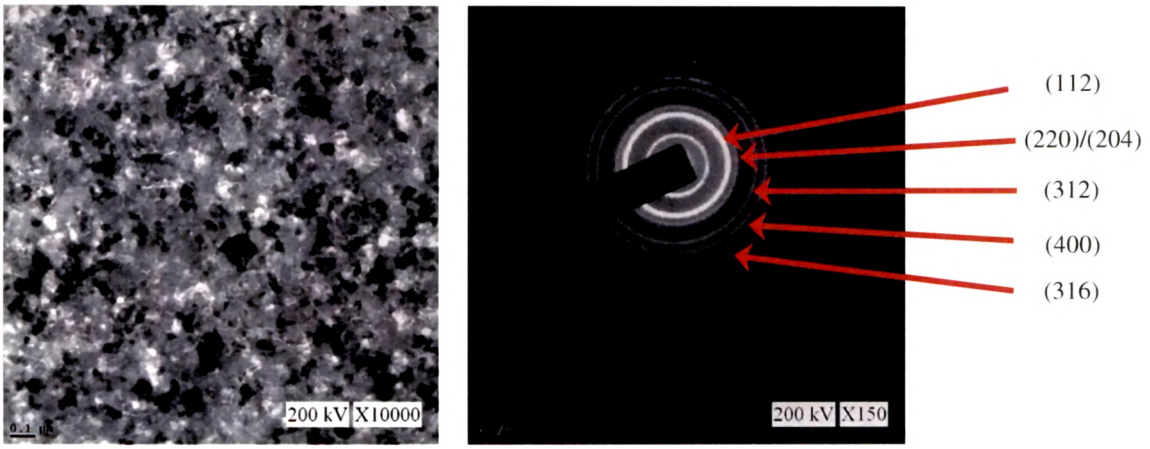

Figure 3.6: TEM image with SAD pattern of CIS film deposited at 523 K.

The SAD pattern contains sharp rings expected for polycrystalline films. It can be noticed that the three characteristic major intensity peaks (112), (220)/(204) and (312) are present in the film. The very prominent bright ring seen in SAD pattern due to the (112) plane indicates the preferred orientation of grains along that direction. All the obtained (hkl) indices of the diffracted rings matched well with those of the JCPDS data (card No.23-209) [95] for chalcopyrite CIS reflections and there are no reflections corresponding to elemental or secondary phases.

3.4.2 Morphological Studies

3.4.2.1 AFM Results

The morphological characteristics of CIS films have been studied using atomic force microscope (AFM) to observe microstructure. The three dimensional (3D) surface topographical images recorded for CIS thin films deposited at different T_s and annealed at 573 K, show that grain size and roughness increase with increasing T_s.

AFM image of the film grown at 473 K reveals a structure with dense grains. The irregular shape of the grains suggests that at low T_s, the kinetic energy is not sufficient for the coalescence of the grains. When T_s is raised to 523 K, the crystalline structure and clear grain boundaries became apparent. Thermal annealing of films at 573 K improves crystallinity.

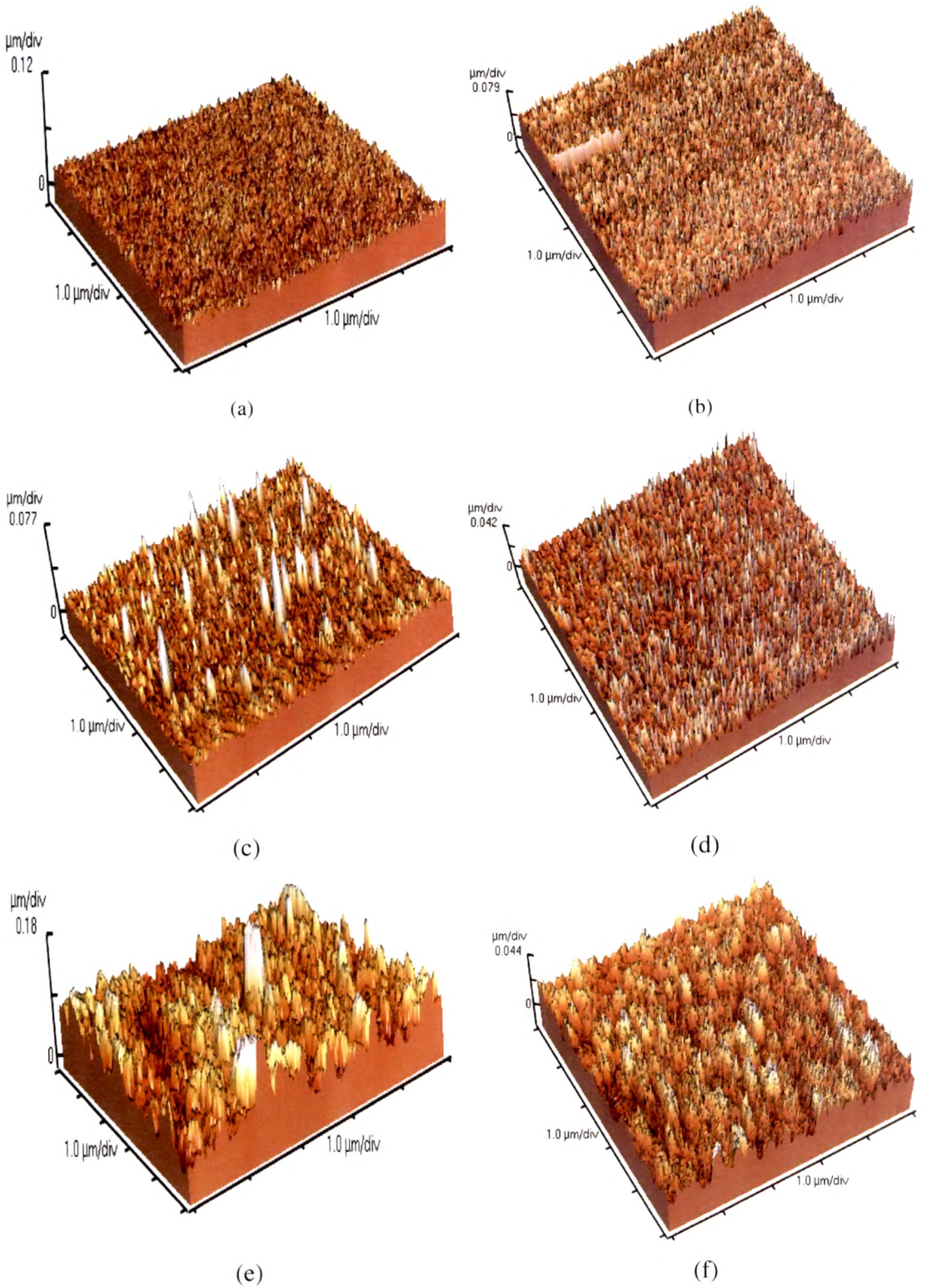

Figure 3.7: Three dimensional AFM images of as-deposited and annealed films grown at different substrate temperature (a) T_s = 473 K, (b) T_s = 473 K and T_a = 573 K, (c) T_s = 523 K, (d) T_s = 523 K and T_a = 573 K, (e) T_s = 573 K, (f) T_s = 573 K and T_a = 573 K.

The temperature dependence of growth and morphology can be explained as follows. The evaporated atoms or molecules arriving on the substrate surface acquire a large thermal energy and hence a large mobility when deposited at higher T_s. This enhances the diffusion distance of the evaporated atoms/molecules. As a result; the collision process initiates the nucleation and enhances the island formation in order to grow continuous films with larger grains.

3.4.2.2 SEM Result

SEM image of CIS thin film deposited at T_s = 523 K is shown in figure 3.8. A non-uniform surface morphology with irregular shaped grains superimposed on smooth flat background material is observed in the film.

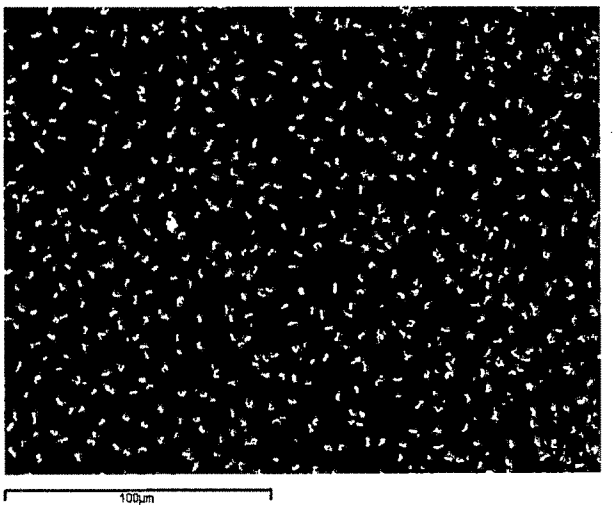

Figure 3.8: SEM image of CIS thin films deposited at T_s = 523 K.

3.4.3 Compositional Analysis of CIS Thin Films

The composition of CIS thin films used as absorbers in thin film solar cell is a topic of main importance since many cell properties are influenced by deviations from stoichiometry. The compositional analysis of the as-deposited samples is carried out with an accelerating voltage of 30 kV using Se_L, In_L, and Cu_K line of the spectrum. EDAX spectrographs of films deposited at different T_s are shown in figure 3.9.

The data of composition for CIS thin films deposited at different T_s is shown in table 3.6.The analysis of composition data of CIS thin films deposited at different substrate temperatures could be described by two parameters non-molecularity Δm and non-

stoichiometry Δs which have been described is section 3.2.2. This is useful to identify primary intrinsic defects in the CIS thin films which are also called native defects, include copper vacancies (V_{Cu}), copper-on-indium (Cu_{In}) antisites, indium-on copper antisites (In_{Cu}), and selenium vacancies (V_{Se}).

Table 3.6: EDAX analysis of CIS thin films grown at different substrate temperatures.

Substrate Temperature (T_s) K	Composition (Atomic weight %)			Molecularity deviation Δm	Stoichiometry deviation Δs
	Cu	In	Se		
473	25.21	27.51	47.28	-0.08	-0.16
523	25.04	25.51	49.45	-0.02	-0.03
573	26.19	27.42	46.39	-0.04	-0.18

The analysis of the data obtained for as-deposited CIS films suggests that for films deposited at different T_s a near stoichiometric composition is found with values of Δm in the range of (-0.02)-(-0.04) while values of Δs is in the range of (-0.03)-(-0.18). Very little change in the value of Δm indicates that T_s has no influence on Cu and In content. As samples are p-type as tested using hot probe method, Cu_{In} substitution defects are most probable in the films.

3.4.4 Optical Transmission Measurements

Optical transmission measurements of CIS thin films deposited at different T_s are carried out in the wavelength range 500 nm-1500 nm at normal incidence using the experimental set up shown in figure 2.9. The data has been analyzed to calculate absorption coefficient of CIS thin films using Lambert's law. The transmission spectra of CIS thin films deposited at different T_s is shown in figure 3.10. Analysis of transmission data suggests that CIS thin film deposited at different T_s have the highest value transmission near the absorption edge suggesting that absorption starts near it. The absorption coefficient of CIS thin films deposited at different T_s, as calculated using Lambert's law is used to calculate energy bandgap. As CIS is a direct bandgap semiconductor it follows the relation,

$$\alpha = \frac{A_0}{h\upsilon}\sqrt{h\upsilon - E_0} \qquad (3.3)$$

Here E_0 is the fundamental optical bandgap energy and A_0 is an edge width parameter.

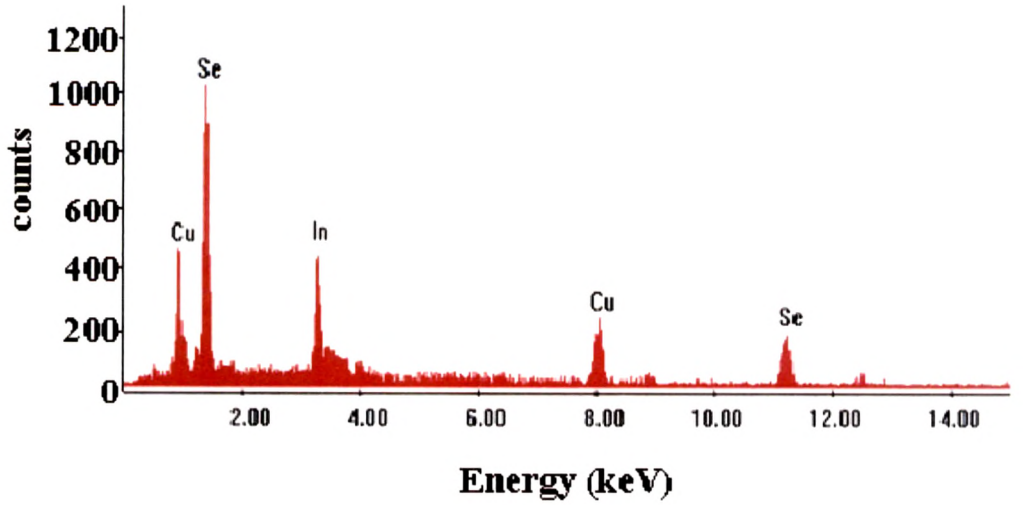

(a)

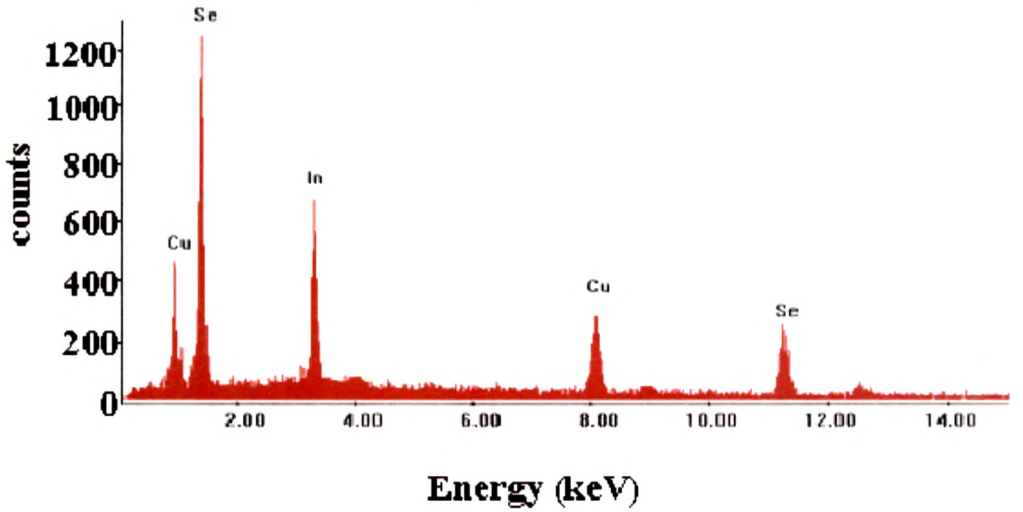

(b)

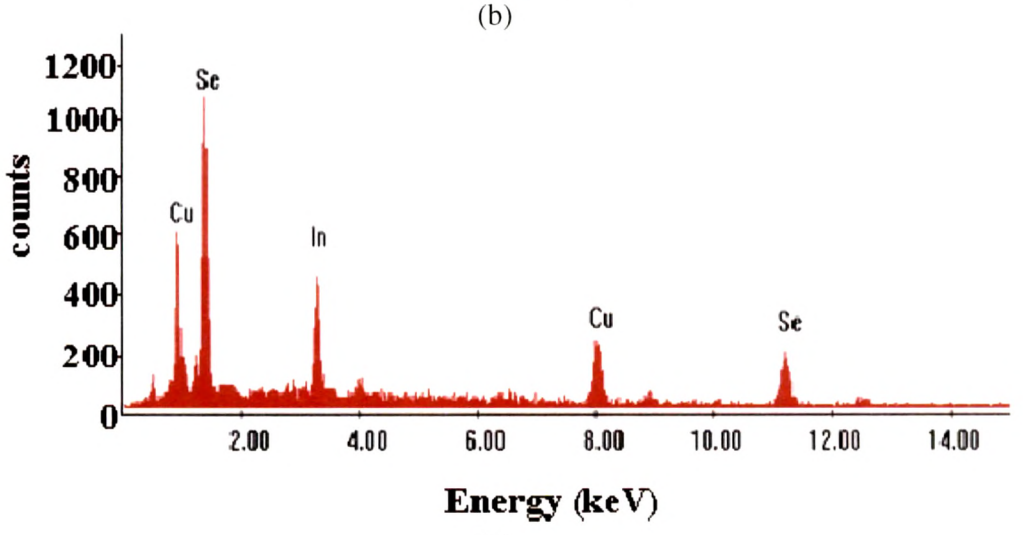

(c)

Figure 3.9: EDAX spectrograph of CIS thin films deposited at a) T_s = 473 K (b) T_s = 523 K (c) T_s = 573 K.

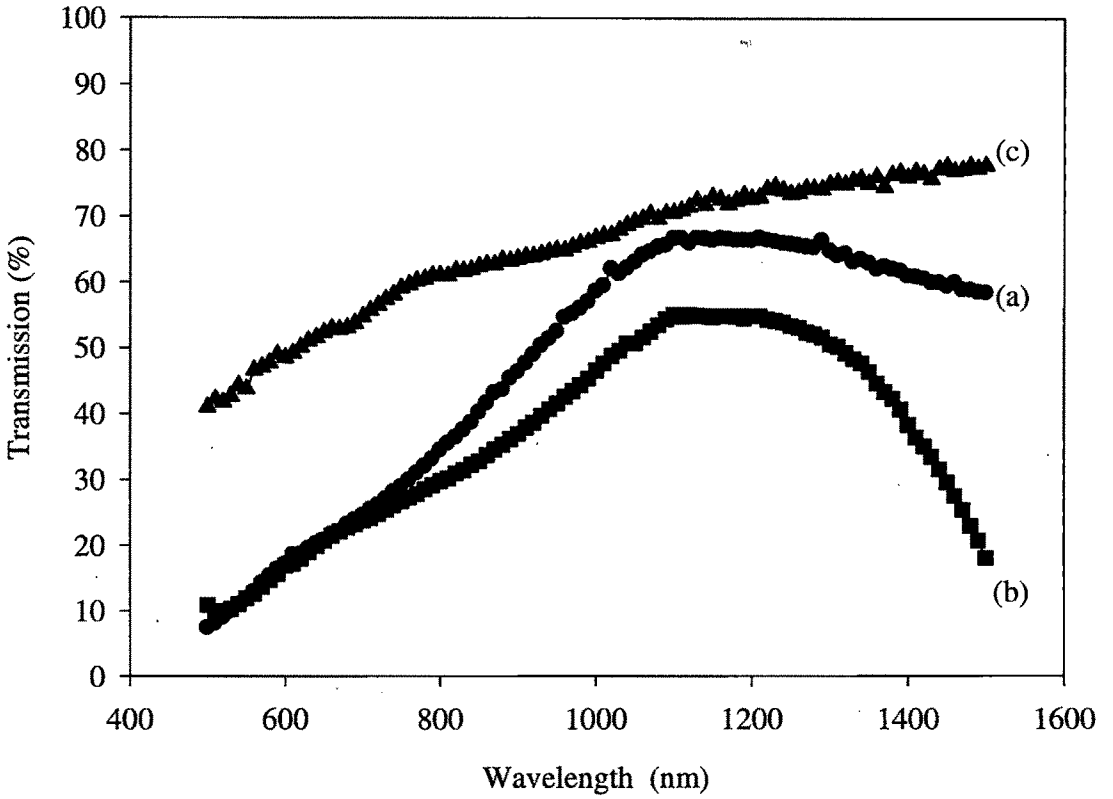

Figure 3.10: Transmission spectra of CIS thin films deposited at different substrate temperatures (a) T_s = 473 K, (b) T_s = 523 K and (c) T_s = 573 K.

Plots of $(\alpha h\nu)^2$ versus $h\nu$ for CIS films deposited at different T_s is shown in figure 3.11. It is observed from the plots that, for $h\nu > 1$ eV the plot of $(\alpha h\nu)^2$ as a function of $(h\nu)$ follows a straight line (fundamental absorption). Hence the energy axis intercept to the linear part yields the energy bandgap of CIS thin films. The nonlinear steps in the energy range $h\nu <$ 1 eV can be attributed to interference due to multiple reflections that take place at the surface and backside of the film. For CIS thin film deposited at different T_s values of energy bandgap are found in the range of 1.01-1.04 eV. These values are in good agreement with the bandgap values as reported by earlier workers [96, 97]. It is clear that as the T_s increases the energy bandgap decreases. This may be due to the sharp edges in the crystalline films. The decrease of bandgap with the increase of T_s is likely to be attributed to an increase of particle size and decrease in strain in CIS thin films [98].

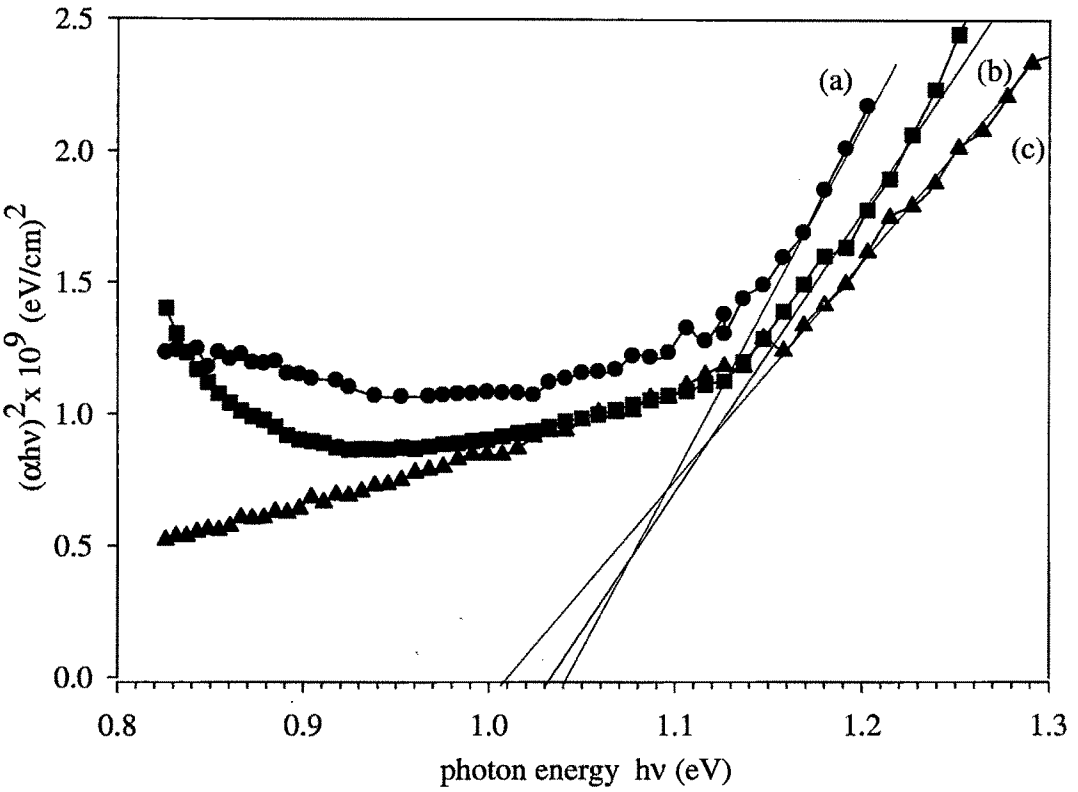

Figure 3.11: Plots of $(\alpha h\nu)^2$ vs hv for CIS films deposited at different substrate temperatures (a) T_s = 473 K, (b) T_s=523 K, (c) T_s = 573 K.

Thermal annealing of CIS thin films at 573 K temperature for films deposited at different T_s reduces energy bandgap. Figure 3.12 shows plots of $(\alpha h\nu)^2$ versus hv for CIS films deposited at different T_s and annealed at 573 K. Decrease in energy bandgap on thermal annealing is consistent with the fact that the crystallinity of the films improve on annealing.

3.4.5 Electrical Characterization

3.4.5.1 Resistivity Measurements

According to literature review, CIS thin films having p-type charge transport mechanism is used as an absorber in solar cells. For electrical characterization performed in this study, non rectifying (ohmic) contact with the investigated film is achieved using silver-paste electrodes. Electrical characterizations of as-deposited and annealed films are carried out using Hall Effect method. The type of electrical conduction in CIS thin film is verified using hot probe method. The data of resistance measurement with T_s suggests that the resistivity increases with increase of T_s suggesting that stoichiometry improves. According to EDAX analysis, we can conclude that film growth at this initial composition takes place in multiphase conditions.

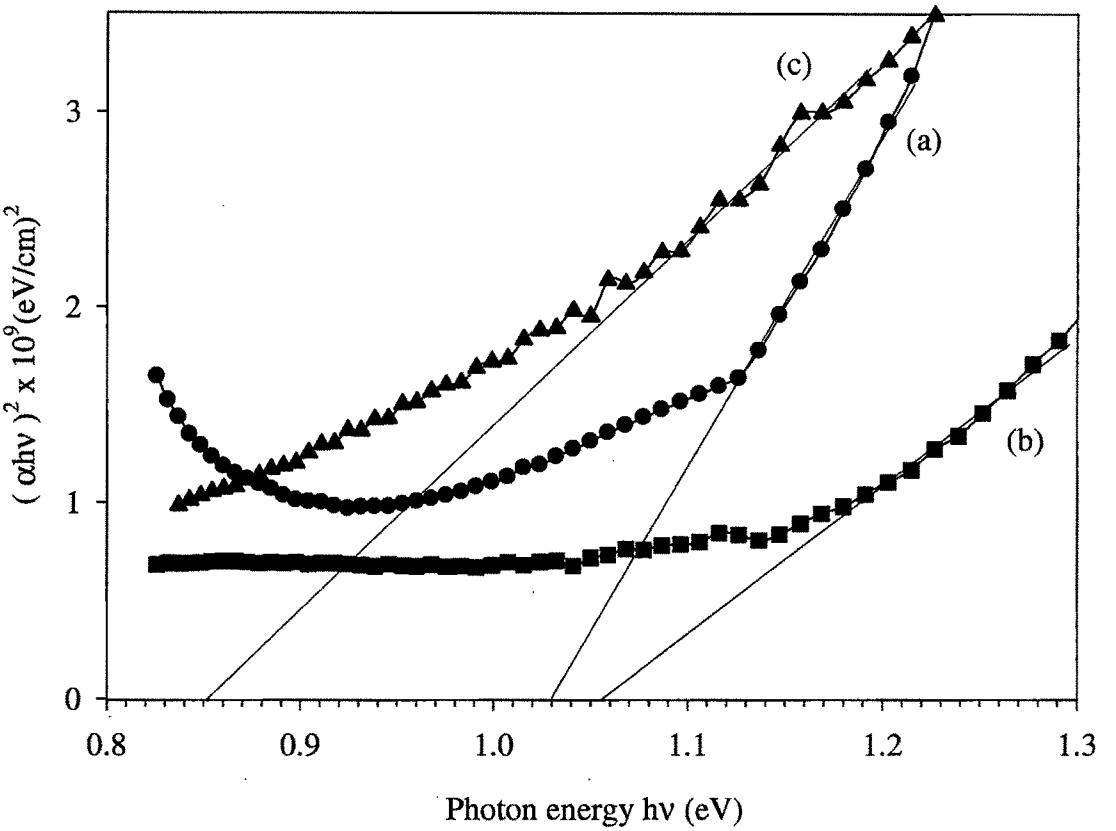

Figure 3.12: Plots of $(\alpha h\nu)^2$ vs hν for CIS films deposited at different substrate temperatures and annealed at 573 K (a) T_s = 473 K, (b) T_s = 523 K, (c) T_s = 573 K.

The electrical parameters derived from the Hall Effect measurements at room temperature are shown in table 3.7. The Hall mobility of the CIS thin films deposited at different T_s decreases when the films are annealed at 573 K at a base pressure of 10^{-2} Torr which is due to increase in point defects. Kazamerski et al. [99] have also observed such a decrease in the Hall mobility when they had annealed CIS thin films for more than 30 min.

Table 3.7: Electrical properties of CIS thin films.

Substrate Temperature T_s (K)	Annealing Temperature T_a (K)	Resistivity ρ (Ω cm)	Mobility μ (cm^2/Vs)	Carrier Concentration p $(cm)^{-3}$
473	Unannealed	0. 59	144	7.2×10^{17}
	573	0.15	14	2.9×10^{17}
523	Unannealed	3.50	141	1.2×10^{16}
	573	0.30	23	8.2×10^{17}
573	Unannealed	18.80	165	2.0×10^{15}
	573	0.02	42	5.8×10^{18}

3.4.5.2 Activation Energy

XRD analysis of CIS thin films deposited at different T_s revealed that the films are polycrystalline in nature, which is further confirmed by TEM analysis of representative film deposited at 523 K. For this reason number of lattice defects such as vacancies, interstitials and antisites is expected to be present in the material. As such defects influence the performance quality of absorber, an analysis of defects in film deposited at different T_s is carried out by an examination of activation energies. This can be done either by photoluminescence or by use of measurements of conductivity σ as a function of temperature (Arrhenius plot). In this work we have followed the second method.

In the literature [100] the temperature dependence of the semiconductor materials conductivity is expressed by the equation,

$$\sigma(T) = \sigma_0 \exp\left(\frac{-E_a}{k_B T}\right) \tag{3.4}$$

where σ_o is the pre-exponential factor, E_a is thermal activation energy, k_B is the Boltzmann constant, T is temperature in Kelvin. The linear-least square fit of plot of $\ln(\sigma)$ versus $10^3/T$ will be straight line from the slope of which the activation energy can be calculated. Arrhenius plot ($\ln\sigma$ vs 1000/T) of DC conductivity (σ) of the film-deposited at 523 K is presented in figure 3.13. From the plot it is clear that the conductivity of the films increases with temperature indicating semiconducting behavior of the samples. The activation energy calculated for films deposited at different T_s and annealed at 573 K is shown in table 3.8.

The activation energy calculated from the linear-least square fit of the Arrhenius plots for CIS thin film deposited at different T_s corresponds to the defect level. As films are not doped intentionally and therefore the defects observed are of an intrinsic nature. As the conductivity of the film is p-type, acceptor-like levels are expected to be present.

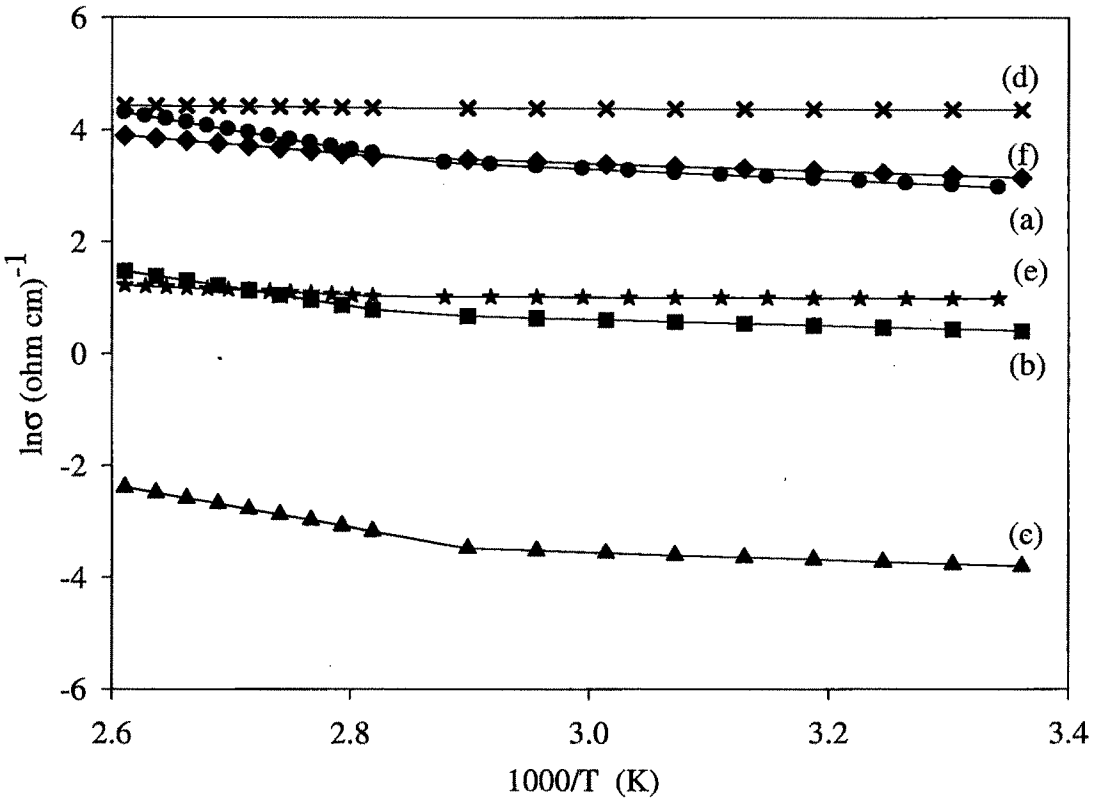

Figure 3.13: Arrhenius plots of CIS thin films deposited at (a) T_s = 423 K, (b) T_s = 523 K, (c) T_s = 573 K, (d) T_s = 423 K and T_a = 573 K, (e) T_s = 523 K and T_a = 573 K, (f) T_s = 573 K and T_a = 573 K.

In CIS selenium vacancies act like donors while selenium interstitials act like acceptors. The activation energies for annealed films are found to decrease. The decrease of the activation energies after heat treatment can be attributed to the increase of grain size leading to a decrease of the density of grain boundaries resulting in a reduction of the inter grain barrier [101]. The values of activation energy correspond well with the measurements performed by other groups for CIS thin films and mono-crystals as well [94, 102, 103].

Table 3.8: Activation energy of as-deposited and annealed CIS thin films.

Substrate temperature T_s (K)	Annealing temperature T_a (K)	Activation Energy E_{a1} (meV)	Activation Energy E_{a2} (meV)
423	Unannealed	302	82
	573	154	42
523	Unannealed	175	56
	573	80	22
573	Unannealed	152	46
	573	67	12

3.5 Deposition of CIS Thin Films using Flash Evaporation Technique

Flash evaporation technique is widely used by researchers to deposit binary/ternary semiconductor compound material owing to its simplicity and ease of operation. In this technique pulverized compound material is transported to an evaporation boat, hot enough to provide a quick evaporation of the material. However, poor reproducibility and compositional deviations are the major problems while depositing ternary compound such as CIS [75]. We have overcome this problem by keeping the boat temperature high enough (~1473 K) and reducing the rate of deposition. Here results obtained from a study on the effects of the T_s on the properties of flash-evaporated CIS films are presented.

3.5.1 Structural Characterization

The XRD patterns carried out for CIS in powder form and thin films of CIS grown at four different T_s viz 300 K, 473 K, 523 K and 573 K is shown in figure 3.14. The analysis of XRD data show that synthesized CIS powder has a polycrystalline nature. XRD peaks at (112), (220)/(204),and (400) indicates the presence of chalcopyrite phase. The absence of XRD peaks due to binary alloy or different phases indicates good structural homogeneity of synthesized CIS powder. The (112) preferred orientation and splitting of peaks due to tetragonal structure demonstrate good crystalline quality.

The XRD pattern of CIS thin film deposited at various T_s indicate that all the films showed an intense (112) preferred orientation of grains except the film grown at 300 K which is amorphous in nature. The intensity of (112) peak has been found to increase with increasing T_s up to 523 K while the full-width at half maximum (FWHM) values of CIS peak decreases showing that the crystalline size increases. For CIS thin film deposited at T_s = 573 K intensity of (112) peak and crystallite size decreases. This is due to change in stoichiometry of film. The mean size of the crystallites in CIS thin films deposited at different T_s is calculated from (112) x-ray diffraction peak broadening using the well-known Scherrer's formula are shown in table 3.9.

Table 3.9: The position of (112) peak, FWHM and crystallite size of the films grown at different T_s.

Substrate Temp. T_s (K)	Position of (112) peak (Degrees)	FWHM (Degrees)	Crystallite size d (nm)
373	27.09	0.469	21
523	26.82	0.350	30
573	27.16	0.789	11

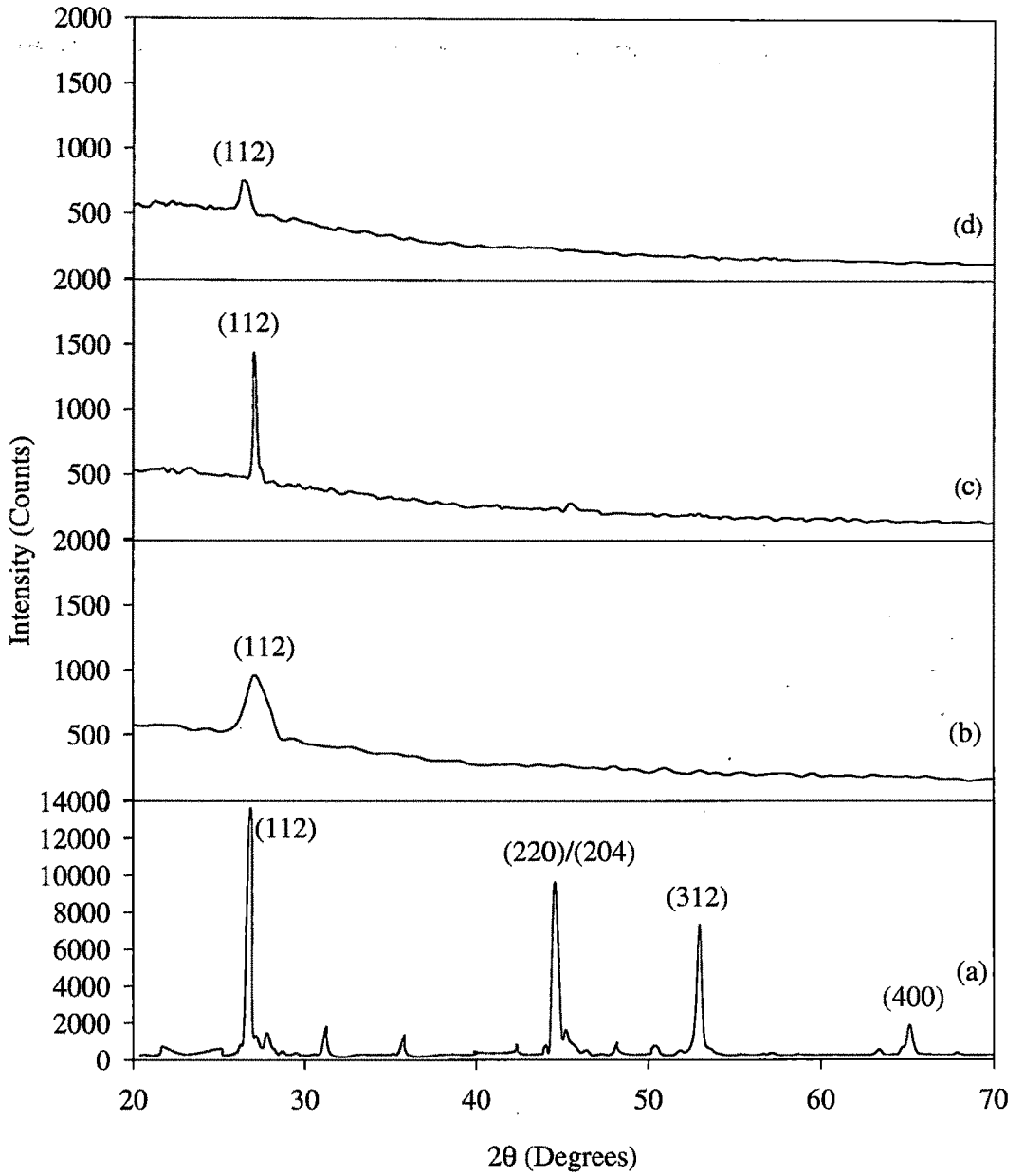

Figure 3.14: XRD pattern of CIS in (a) Powder form and thin films deposited at, (b) T_s = 373 K, (c) T_s = 523 K, (d) T_s = 573 K.

3.5.2 Morphological Studies

3.5.2.1 AFM Results

The surface morphology of CIS thin films grown at three different T_s is studied using AFM to observe microstructure. Figure 3.15 shows the surface topographical images recorded for CIS films deposited at different substrate temperatures.

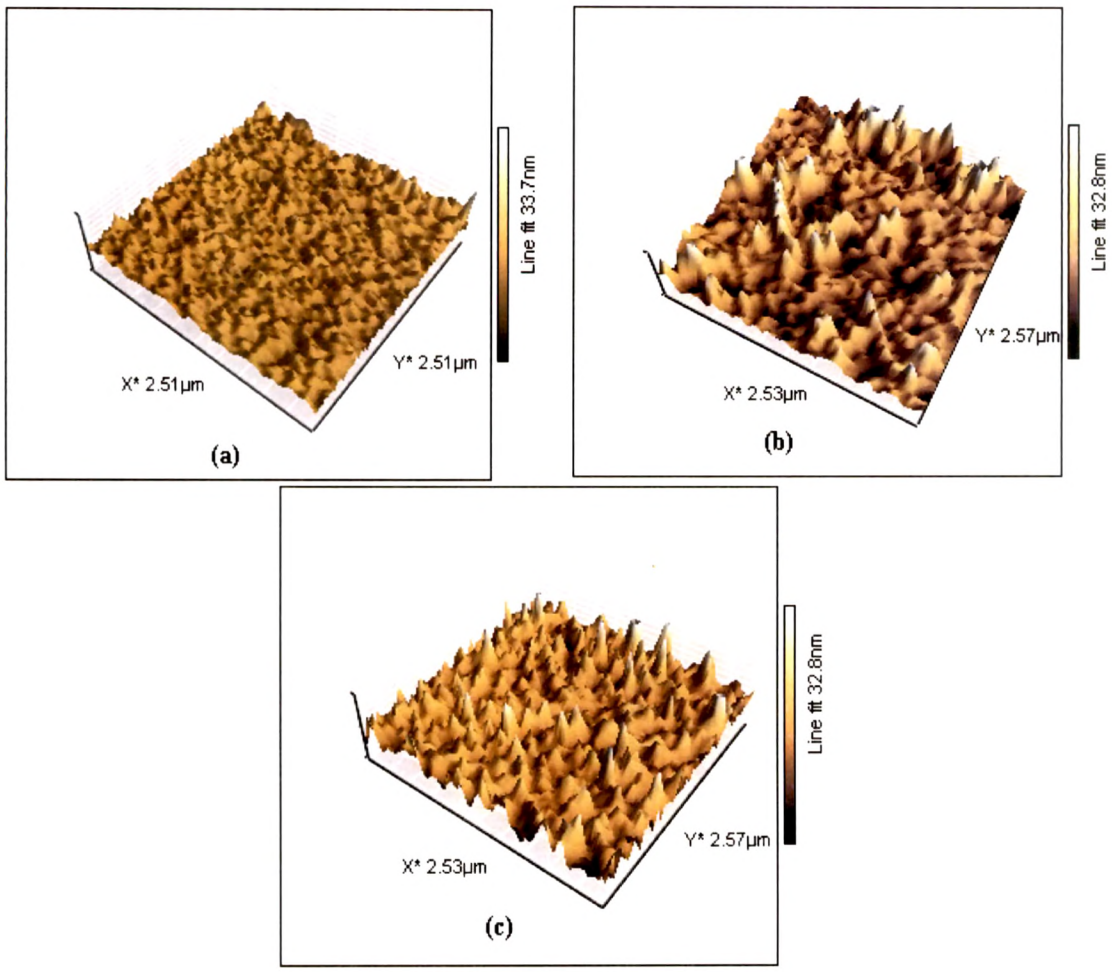

Figure 3.15: AFM images (3-dimensional) of the films grown at, (a) T_s= 373 K, (b) T_s = 523 K, (c) T_s = 573 K.

AFM image of the film grown at 373 K reveals a structure with dense grains. The root mean square (rms) roughness is 2.14 nm. The surface topography is composed of clusters of varying sizes with irregular shapes. The irregular shape of the grains suggests that at low T_s the kinetic energy is not sufficient for the coalescence of the grains. When T_s is raised to 523 K, the crystalline structure and clear grain boundaries became apparent. The rms roughness values of the CIS films grown at 523 K and 573 K are 5.75 nm and 4.84 nm respectively.

3.5.2.2 SEM Results

As revealed by AFM, the as-deposited films have typically a rough surface due to island-like precipitates on the film surface. It is very interesting and important to clarify the composition of the surface segregation with respect to the matrix. With integrated EDAX function, SEM is very powerful tool for observation and identification of the surface segregation. SEM images of CIS films deposited at three different substrate temperatures. is shown in figure 3.16.

3.5.3 Compositional Characterization

The composition of CIS is a topic of main importance since many cell properties are influenced by deviations from stoichiometry [104]. The typical EDAX spectrum of CIS films deposited at different substrate temperatures is shown in the figure 3.17. Table 3.10 shows the data of elemental composition of CIS thin films deposited at different substrate temperatures.

Table 3.10: EDAX analyses of synthesized CIS thin films grown at different substrate temperatures.

Substrate Temperature T_s K	Elemental Composition (Atomic Weight %)			Ratio Cu/In	Se/M*
	Cu	In	Se		
373	25.96	26.32	47.72	0.98	0.90
523	25.94	24.82	49.24	1.04	0.97
573	22.72	27.70	49.58	0.82	0.98

*M= [Cu] + [In]

It is clear that elemental composition approaches close to stoichiometry (i.e.1:1:2) with increase in T_s. CIS thin films deposited at T_s = 523 K has near stoichiometric composition of elements.

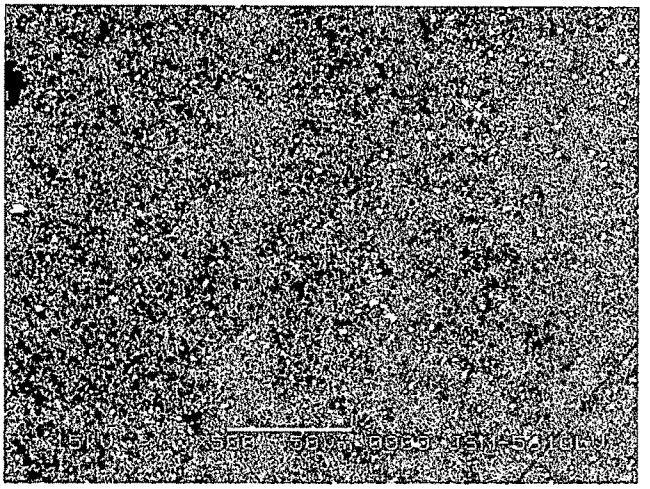

(a)

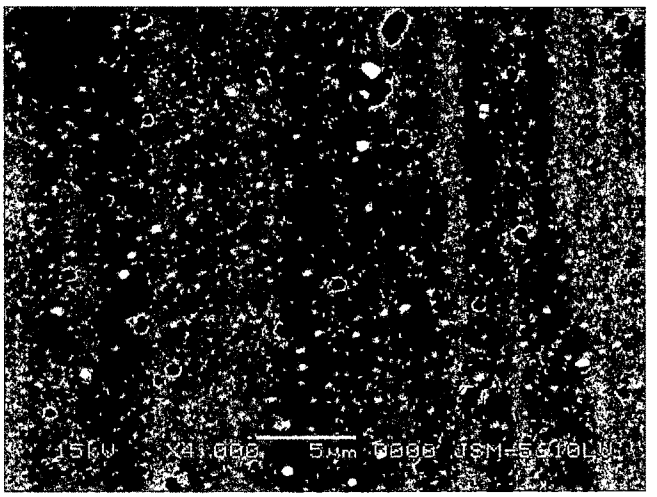

(b)

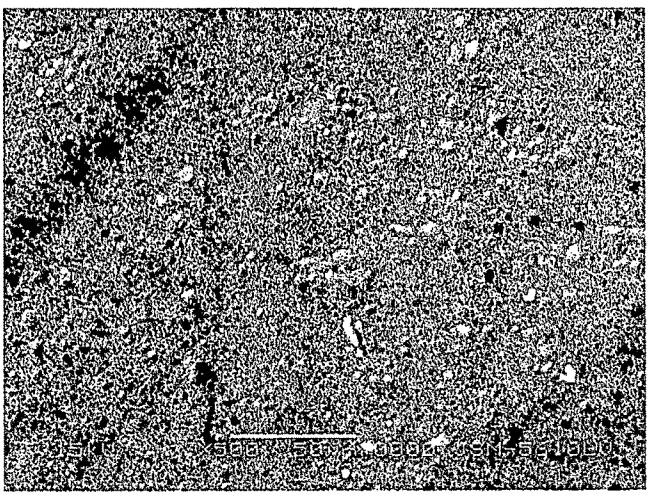

(c)

Figure 3.16: SEM images of CIS films deposited at different substrate temperatures, (a) T_s = 373 K, (b) T_s = 523 K, (c) T_s = 573 K.

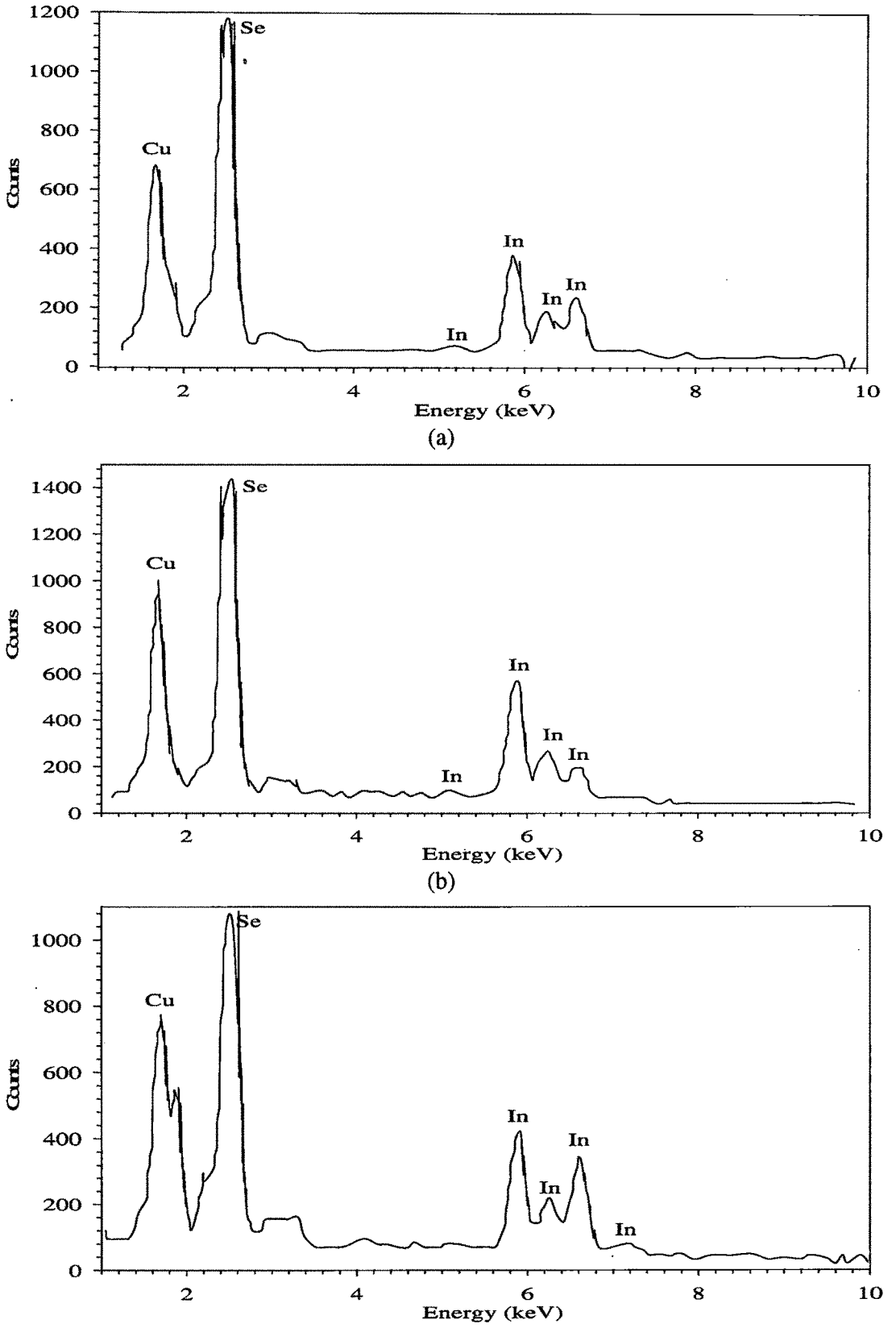

Figure 3.17: EDAX pattern of CIS films deposited at three different substrate temperatures (a) T_s = 423 K, (b) T_s = 523 K, (c) T_s = 573 K.

3.5.4 Optical Transmission Measurements

The variation of transmittance, T, as a function of wavelength for CIS thin films of ~200 nm thickness deposited at different T_s is shown in the figure 3.18

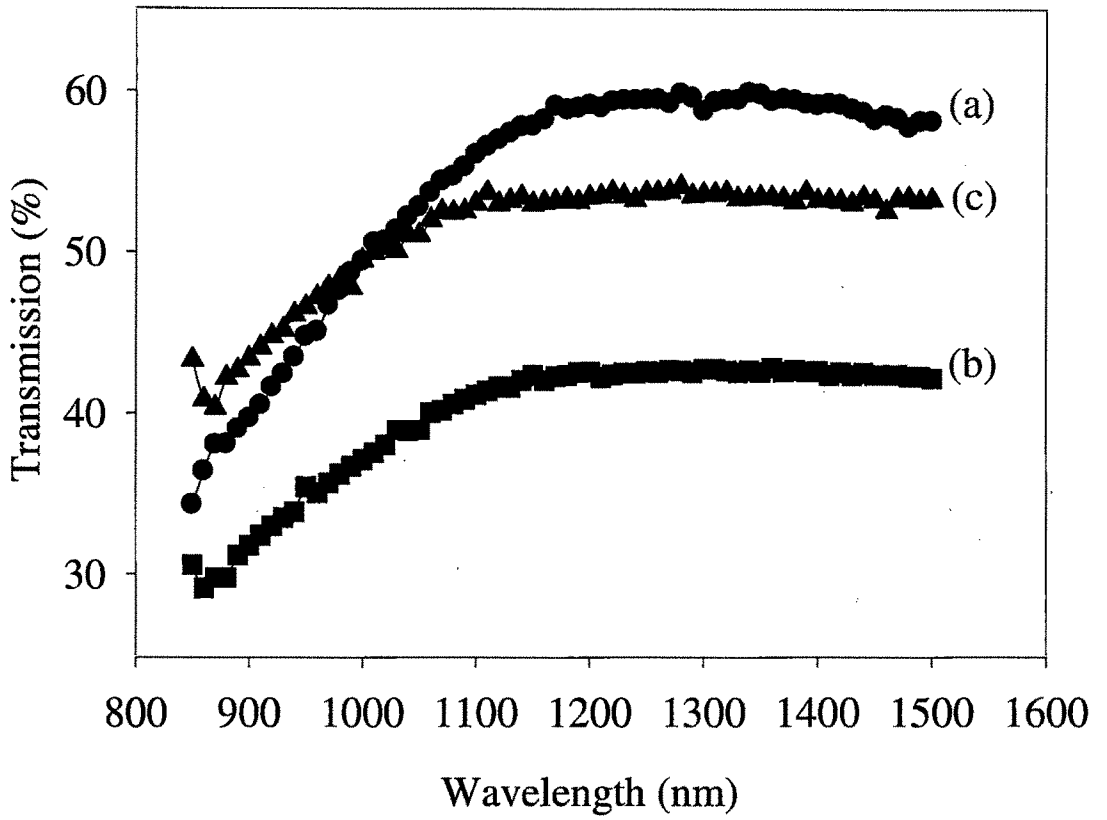

Figure 3.18: Spectral variation of transmission of films deposited at (a) T_s= 373 K, (b) T_s = 523 K, (c) T_s= 573 K.

It is observed from the transmission spectra that all films have transmittance of 20 % to 60 % in the wavelength range 800 nm-1500 nm depending on T_s. The peak values of transmission spectra are seen at around 1100-1200 nm suggesting that the absorption starts around this wavelength. In the near infrared, the transmittance is observed to be less dependent on photon energy above 1200 nm. The decrease of transmission in the higher photon energy region is due to free carrier absorption.

The absorption coefficient (α) is calculated from the experimental measured values of transmittance T using the Lambert's law. As CIS is a direct bandgap semiconductor α follows the relation as mentioned in equation 3.3.The plots of $(\alpha h\nu)^2$ with photon energy $h\nu$ for films grown at different T_s is shown in figure 3.19.

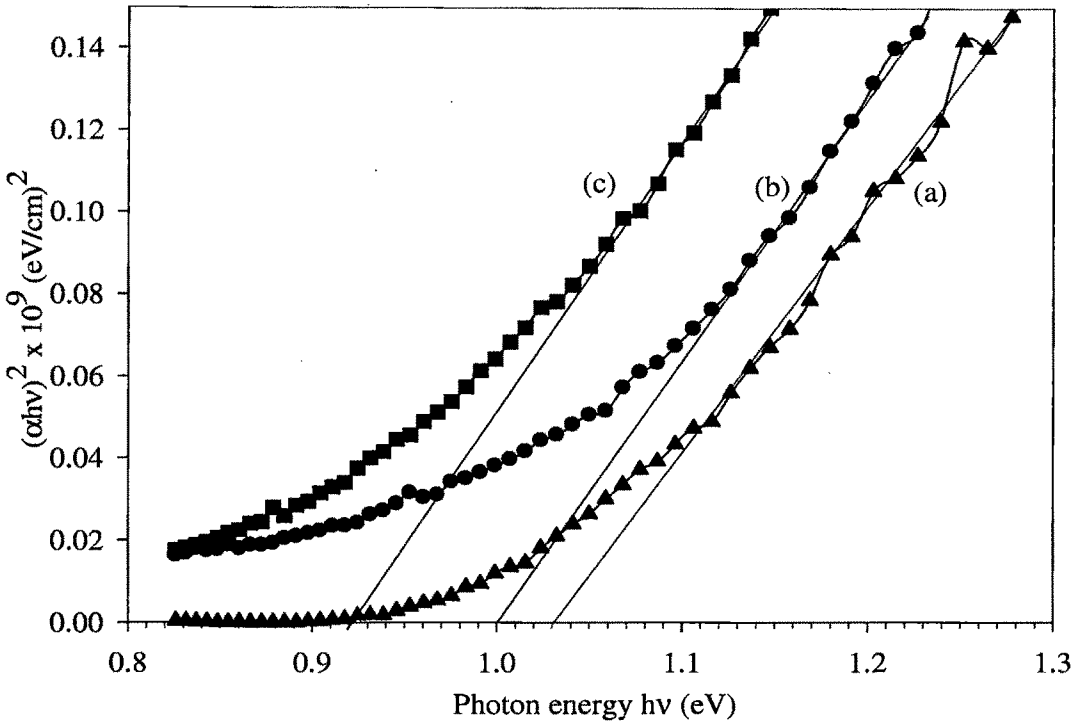

Figure 3.19: Plots of $(\alpha h\nu)^2$ vs hν for films deposited at (a) T_s= 373 K, (b) T_s = 523 K, (c) T_s= 573 K.

Extrapolation of the linear portion of the curve to $(\alpha h\nu)^2 = 0$ gives the bandgap energy which is in the range 0.92-1.03 eV. The bandgap values of this study are in good agreement with the bandgap values by many earlier works [97,105].

3.5.5 Electrical Characterization

A better understanding of the electrical properties of CIS thin films are required for using it as an absorber layer in CIS thin film solar cell. Hall effect measurements of the as deposited films of 200 nm thickness are carried out using silver paste as contact material. Figure 3.20 shows variation in resistivity and mobility of the films grown at different substrate T_s. From the graph, it is clear that as the substrate temperature increases mobility increases. This is due to increase in crystallite size as observed in XRD analysis. The increased crystal size weakens the intercrystalline boundary scattering and increases the carrier lifetime, consequently increasing the mobility.

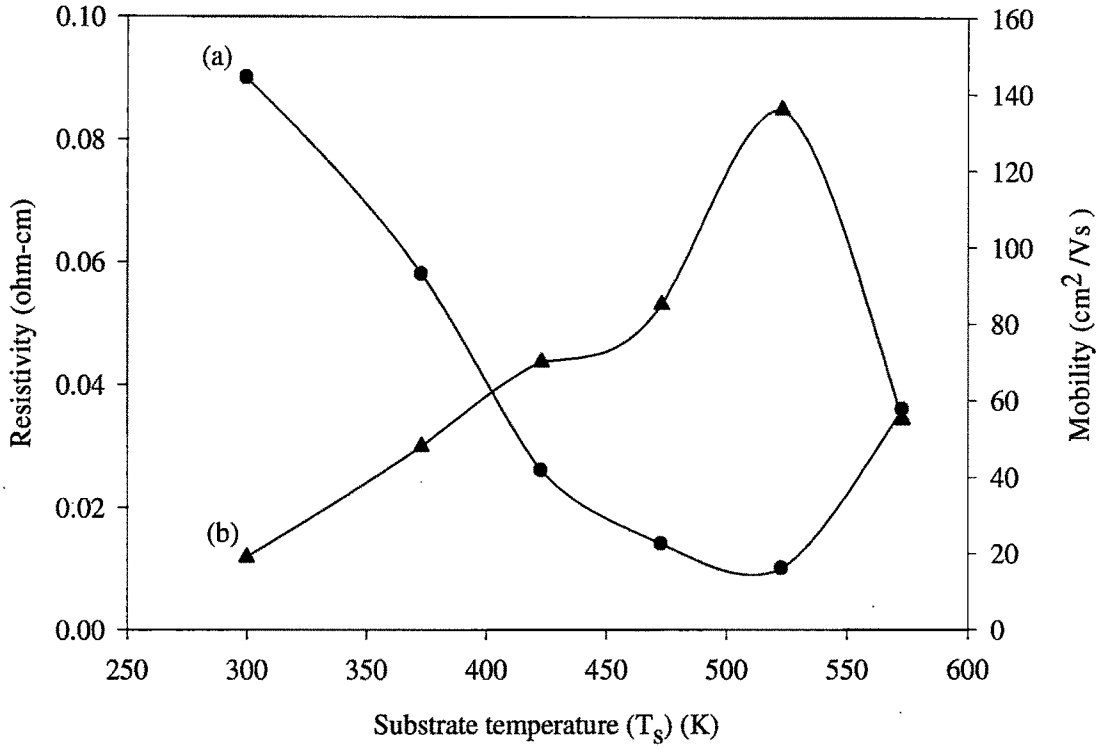

Figure 3.20: Variation of (a) resistivity (b) mobility with substrate temperature.

The decrease in resistivity with the increase in substrate temperature can be explained using Petritz's barrier model [106]. According to which at low temperatures, the crystallites do not grow sufficiently large while at higher substrate temperature large crystallite sizes are obtained which ultimately decrease the intercrystalline barrier, therefore have to cross comparatively narrow intercrystalline barriers and this result in decrease of resistivity. The resistivity of the films deposited at 573 K substrate temperature increased rapidly which may be due to the saturation of the grain size. All films had p type conductivity as identified by the hot probe method and carrier concentration in the range 10^{17}-10^{18} cm^{-3}.

CIS thin film deposited at substrate temperature of 523 K shows good structural and optical property as indicated by XRD, AFM and transmittance measurements. To observe the changes in the electrical property with thickness we have deposited films of different thicknesses (from 200 nm-500 nm) at a substrate temperature of 523 K. Figure 3.21 shows the measured electrical resistivity of CIS films.

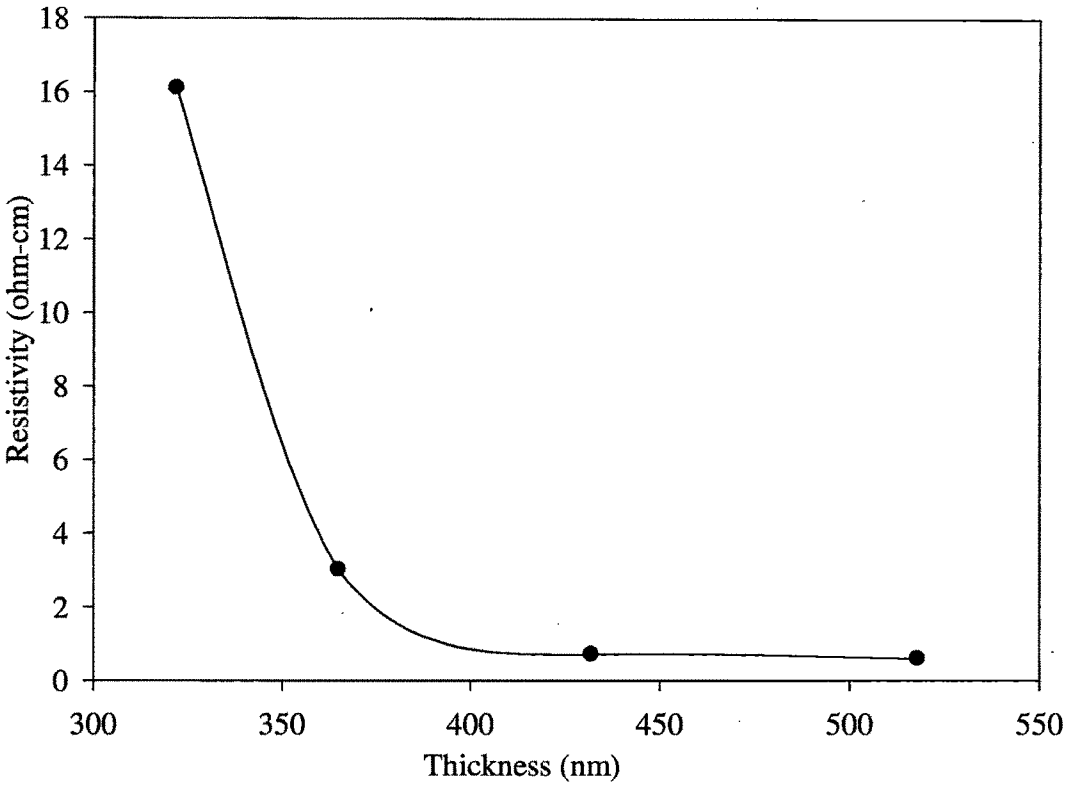

Figure 3.21: Resistivity variation with thickness.

Decrease in resistivity with thickness can be interpreted on the basis of grain boundary scattering as discussed by Wu-et.al. [107]. As the thickness increases, the grain size increases, grain boundary size becomes relatively reduced that in turn reduces grain boundary scattering and increases the carrier life time, consequently reducing the resistivity.

3.5.6 Activation Energy

Arrhenius plot of $\ln(\sigma)$ versus $10^3/T$ of CIS film deposited at 523 K substrate temperature is shown in the figure 3.22. For that, we have studied temperature dependence of resistance of CIS thin films of ~200 nm thickness prepared on soda lime glass substrate. The samples are heated without illumination in the temperature range of 300-400 K while the resistance is continually measured. The activation energy calculated from linear-least square fit of Arrhenius plot is ~30 meV. In the temperature range studied CIS thin film exhibited a thermally activated electrical conductivity and conduction process is governed by grain boundaries. Activation energy calculated agrees quite well with the reported values [87] for CIS film prepared using stacked elemental layers.

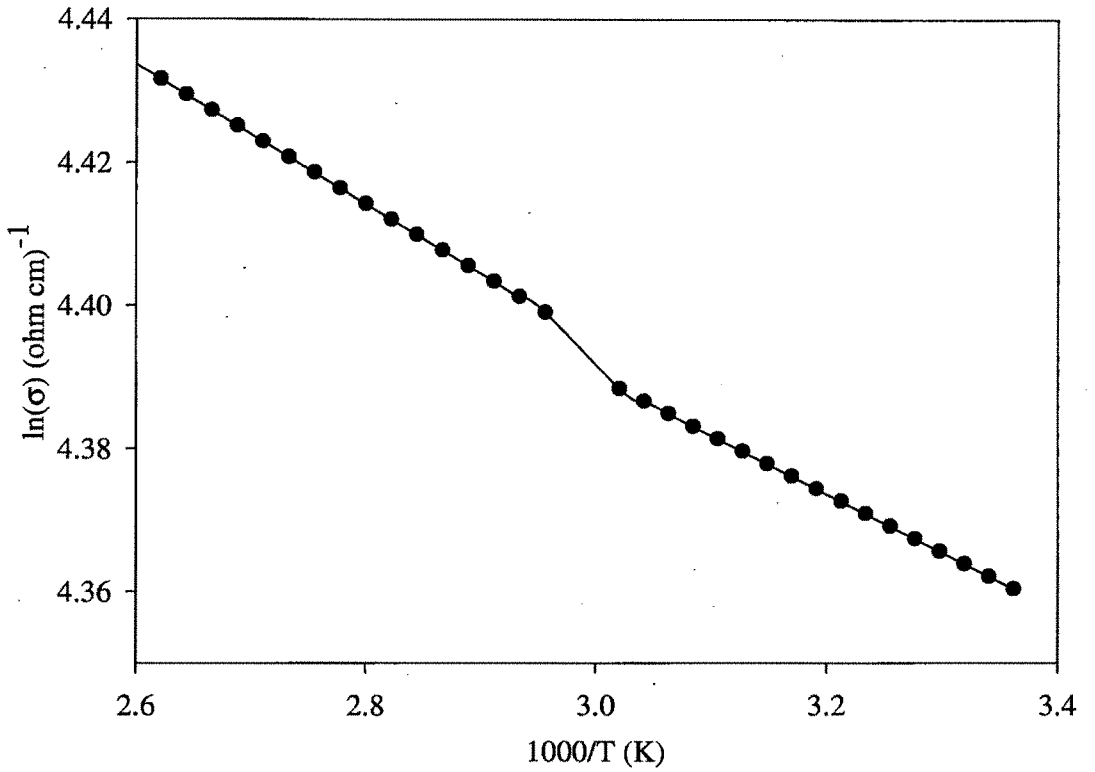

Figure 3.22: Arrhenius plot for the film deposited at 523 K.

Conclusions

CIS thin films have been deposited on soda lime glass substrates from synthesized pulverized compound material by two different deposition techniques viz. thermal evaporation and flash evaporation.

It is concluded that, by controlled increase in source temperature CIS thin films are prepared by thermal evaporation of synthesized stoichiometric compound material at different T_s, followed by thermal annealing at 573 K in a vacuum coating unit at base pressure of 10^{-2} Torr. Structural analysis of CIS thin films revealed that the T_s and thermal annealing has significant effect on structural properties of films. EDAX measurements of films revealed a near stoichiometric composition of elements for T_s not exceeding 523 K. For higher T_s a drop in Se content is observed, indicating a re-evaporation of Se and leading to a reduction in film quality. The electrical resistivity obtained from Hall Effect measurements are in the range 10^{-2}-10^{1} Ω cm, indicating the influence of T_s and thermal annealing. The activation energies calculated from Arrhenius plots are found to decrease after thermal annealing.

Thin films of CIS are also deposited using flash evaporation technique on glass substrates held at different T_s from synthesized stoichiometric compound material. XRD and AFM analysis revealed that the T_s has significant influence on structural and morphological property of films. EDAX measurements of films revealed a near stoichiometric composition of elements. The electrical resistivity obtained from Hall effect measurements were in the range 10^{-2} Ω cm influenced by substrate temperature. Analysis of optical transmission measurements of CIS films deposited different substrate temperatures revealed value of E_g in the range 0.92 -1.03 eV. Absorption coefficient α greater than 10^4 cm^{-1} is observed for all films. Activation energy calculated from temperature dependent electrical conductivity measurements of CIS thin film deposited at 523 K is 30 meV.